Nuclear magnetic resonance (NMR) properties of unconsolidated sediments in field and laboratory

Martin Müller[*], Stefan Kooman and Ugur Yaramanci

TU Berlin, Dept. of Applied Geophysics, Ackerstrasse 71-76, 13355 Berlin, Germany

ABSTRACT

Surface nuclear magnetic resonance (SNMR) is a geophysical technique that has proved to be a useful tool for the investigation of hydrological properties of aquifers (porosity ϕ, saturated hydraulic conductivity k_f) in the past 10–15 years. Until recently, laboratory NMR has focused on consolidated sediments. In this research, an attempt is made to investigate unconsolidated sediments. To enable an enhanced understanding and interpretation of SNMR data, laboratory nuclear magnetic resonance (NMR) properties of synthetic and natural unconsolidated samples (glass beads, sand mixtures, bore-core samples from a Quaternary environment west of Berlin (Germany) and coarse sand samples with a varying clay content) were analysed. To verify the NMR measurements, pore-space properties (specific surface, porosity, pore-size distribution) were analysed. Finally, hydraulic conductivity measurements were conducted to verify both the hydraulic conductivity derived from NMR relaxation times and the hydraulic conductivity estimates based on grain size. The laboratory data were compared to SNMR field data to assess scaling effects due to the dispersion of relaxation.

The results show that the relationship used to obtain hydraulic conductivity from NMR relaxation is suitable for predicting the saturated hydraulic conductivity of samples composed of clay, silt and coarse sand. Furthermore, it is found that the predictions of hydraulic conductivity of intermediate grain sizes with differing clay content vary over a wide range. A more individual approach with regard to the paramagnetic properties of the material might be needed to achieve successful estimations.

Clay (because of its high specific surface and large surface-to-pore-volume (S/V) ratio) has a strong influence on NMR relaxation and the associated saturated hydraulic conductivity. The NMR relaxation of a series of coarse sand samples (d=1.0–0.5 mm) with a clay content in the range 3–20% shows an exponential decay for the hydraulic conductivity.

INTRODUCTION

The nuclear magnetic resonance (NMR) technique is used in geophysics mainly for well logging and laboratory applications. The advantage of NMR is based on its direct sensitivity to water-protons (^{1}H). Furthermore, structural parameters, such as porosity, pore-size distribution and permeability, of porous media can be determined by NMR (Sen *et al.* 1990; Kenyon 1997; Straley *et al.* 1997). In recent years, surface NMR (SNMR, or magnetic resonance sounding (MRS)) has been used for hydrogeological applications (e.g. Shirov *et al.* 1991; Legchenko and Shushakov 1998; Legchenko and Beauce 1999; Yaramanci *et al.* 1999; Legchenko and Valla 2002). The need for well-founded interpretation of MRS/SNMR field data has greatly increased interest in the NMR properties of sediments (Yaramanci *et al.* 1999; Müller *et al.* 2002). Efforts have also been made to compare laboratory data to field data (Yaramanci *et al.* 2002).

As the magnetic field of the earth is used as primary field, SNMR relies on a different field strength from that used in the laboratory. The Larmor frequencies encountered are 0.8–3 kHz in the earth's magnetic field (2 kHz in central Europe), typically some hundred (200–500) kHz in well-logging NMR, and 2–900 MHz in laboratory NMR. The transferability of the laboratory results to field investigations is of great importance for the interpretation of SNMR in terms of hydraulic conductivity or water content. An analysis must, therefore, consider the frequency dependence or dispersion of the relaxation for transferability. At higher precession frequencies, i.e. higher magnetic field strengths, the relaxation time of the longitudinal magnetization T_1 can be as much as twice the relaxation time of the transverse magnetization T_2, whereas at lower frequencies T_1 equals T_2 (Bené 1980). The questions which have to be answered are:

- Is it true that T_1 equals T_2 at typical values of the earth's magnetic field (equivalent to 0.8–3 kHz precession frequency)?
- How strong is the dephasing of the transverse magnetization

[*] mamue@geophysik.tu-berlin.de

of the individual spins due to field gradients which corresponds to an observed relaxation time T_2^* (i.e. $<T_2$)? Is $T_2^* \approx T_2$ in SNMR?

- Can decay times derived from SNMR be compared directly to laboratory NMR decay times? If not, are there any relationships or estimates that can assist the hydrogeological interpretation of SNMR data and models?
- What is the most reliable way to interpret NMR parameters in terms of hydrological parameters, and also regarding dispersion effects?

To assist the understanding of the results we first give an overview of the basics of NMR, and the relevant pore-space properties in terms of water content and hydraulic conductivity as well as their connection to the parameters measured with NMR.

BASICS
Pore-space properties
Porosity
The porosity ϕ is the fraction of the total volume occupied by pores. Pores provide most of the volume available for fluid and/or gas storage. The pores are usually connected to each other by smaller spaces called pore throats (Schön 1996). Two kinds of porosity are defined here:

- The total porosity ϕ_{tot} is the ratio of the volume of the pore space V_{por} to the total volume (volume of matrix and pores), which is also called the bulk volume V of the sample. It can be written:

$$\phi_{tot} = \frac{V_{por}}{V} \tag{1}$$

and also

$$\phi_{tot} = 1 - \frac{V_{mtx}}{V}, \tag{2}$$

where V_{mtx} is the volume of the matrix (volume of grains).
- The effective porosity ϕ_{eff} is the ratio of the volume V_{eff} of the pore space that is interconnected (available for physical processes and available for fluid flow) to the bulk volume V of the sample. It can be written:

$$\phi_{eff} = \frac{V_{eff}}{V} = 1 - \frac{V_{mtx} + V_{iso}}{V}, \tag{3}$$

where V_{iso} is the pore volume that is isolated from the rest of the pore space (i.e. not connected with other pores).

Specific internal surface
The specific internal surface S_{por} is defined as the ratio of the total internal surface S [m^2] of the pores to the pore volume V_{por} [m^3]. This and several other types of specific surface are used (Schön 1996):

- $S_{tot} = S/V$ [1/m]: S relative to the total rock volume;
- $S_{por} = S/V_{por}$ [1/m]: S relative to the pore volume;
- $S_{mtx} = S/V_{mtx}$ [1/m]: S relative to the volume of the solid matrix;
- $S_m = S/m_{mtx}$ [m^2/kg]: S relative to the mass of the matrix.

S_{tot} can be expressed as

$$S_{tot} = \phi_{tot} S_{por} = (1 - \phi_{tot}) S_m. \tag{4}$$

For this work we determined S_{por} with nitrogen adsorption (BET).

Irreducible water content
The non-mobile water content consists of two parts: (1) the adhesive water $V_{w,adhesive}$ or irreducible water $V_{w,irr}$ which is bound to the internal surface S, and (2) the capillary water $V_{w,capillary}$. The irreducible water volume $V_{w,irr}$ is the fraction of the water in a pore that remains bound to the surface of the pore wall when underpressure is applied (by centrifuging), and $V_{w,capillary}$ is removed.

Permeability/hydraulic conductivity
The flow of water through porous media is given by Darcy's law (Bear 1972), i.e.

$$v = -\frac{k}{\eta} \nabla p \quad [\text{m/s}], \tag{5}$$

where v [m/s] is the flow rate, η [kg/ms] is the dynamic viscosity, k [m^2 or 1/μm^2] is the permeability and ∇p [Pa/m] is the hydraulic pressure gradient. In practice, k is expressed in the (non-SI) unit, darcy (1 darcy = 1 d = 9869×10^{-13} m$^2 \approx 1$ μm^2). In hydrogeology with water as the fluid and a given difference in the water levels, (5) is written in its finite form,

$$v = -\kappa \frac{\Delta h}{\Delta x} \quad [\text{m/s}], \tag{6}$$

where ∇h [m] is the hydraulic head difference over a distance Δx [m], and κ (often referred to as k_f) is the hydraulic conductivity [m/s]. For water, 1 md $\approx 10^{-8}$ m/s or 1m/s $\approx 10^5$ d.

The hydraulic conductivity or the permeability can be estimated if some characteristics of the porous media are known. In this work, two models suited for sediments are used:

- The model of Kozeny–Carman (after Schön 1996):

$$k = \frac{\phi_{eff}}{2 T S_{por}^2} \quad [\text{m}^2], \tag{7}$$

where T is the tortuosity, which depends on the square of the ratio of effective path length to the shortest path length and on the constrictivity of the pores.
- The model of Hazen (Hölting 1989):

$$\kappa = C d_{10}^2 \quad [\text{m/s}], \tag{8}$$

where $C = (0.7 + 0.03 T_C)/86.4$ (T_C denotes temperature in degrees Celsius) is an empirical pre-factor and d_{10} is the grain diameter of the first percentile of the grain-size distribution curve. As clay is the main factor in binding water molecules, it can be used to predict the intrinsic permeability (Schön 1996).
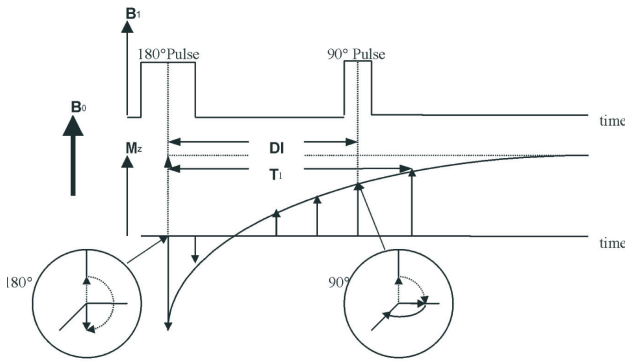
FIGURE 1

INVREC pulse echo sequence to measure T_1. At time zero, a 180° pulse is generated. After a time DI, this is followed by a 90° pulse. The 90° pulse is necessary to turn the magnetization into the xy-plane for signal detection. This sequence is repeated for increasing DI until T_1 is reached (after Abragam 1983).
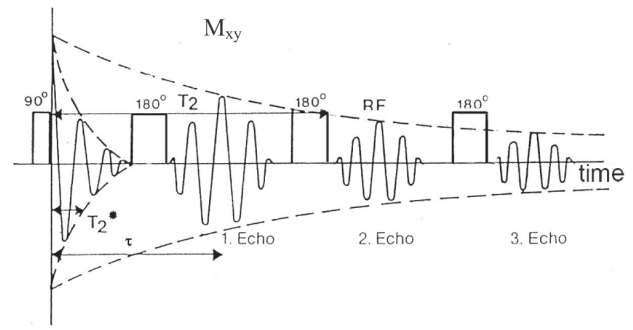

FIGURE 2

CPMG pulse echo sequence to measure T_2. Initially, a 90° pulse is generated and the signal decays with T_2^* (FID). After a certain time, a 180° degree pulse is applied which leads to an echo after the time τ. This sequence is repeated n times until the echoes vanish. The wrap of the echo peaks is the undisturbed T_2 (after Abragam 1983).

Nuclear magnetic resonance

NMR is observed when the nuclei (i.e. protons) of atoms with a magnetic spin are placed in a static magnetic field B_0. At equilibrium (without a secondary field), the net magnetization vector is along the direction of the static magnetic field B_0 (Fig. 1) and is called the equilibrium magnetization M_z or the longitudinal magnetization (Abragam 1983). If the nuclei are exposed to a secondary oscillating magnetic field B_1, the fraction $B_{1\perp}$ which is perpendicular to B_0 causes the magnetization to flip into the xy-plane. The relaxation time T_1 describes how fast M_z returns to its equilibrium value M_z^0 (Fig. 1), where

$$M_z = M_z^0 \, (1\text{-}\exp^{-t/T_1}). \tag{9}$$

The time constant which describes the return to equilibrium of the transverse magnetization M_{xy}, is the relaxation time T_2 (Fig. 2), where

$$M_{xy} = M_{xy}^0 \exp^{-t/T_2}. \tag{10}$$

The net magnetization in the xy-plane decays while the longitudinal magnetization increases up to M_z^0 along z. Therefore, T_2 is always less than or equal to T_1. Hitherto, T_2 has been introduced to describe the transverse relaxation in a homogeneous magnetic field. In addition, the magnetization in the xy-plane starts to dephase because each of the spins experiences a slightly different magnetic field and rotates at its own Larmor frequency. The longer the elapsed time, the greater the phase difference. This leads to the faster decay time T_2^*. To measure T_1, T_2^* or T_2, particular types of pulse sequences (of the secondary magnetic field) can be applied. The most common are: a single 90° pulse or free induction decay (FID) for T_2^*, echo trains of 180° pulses or CPMG (after Carr, Purcell, Meiboom and Gill) for T_2 (see Fig. 2) or a combination of 90° and 180° pulses (inversion

recovery, INVREC) for T_1 (see Fig. 1).

For a free fluid, T_1 is also called the spin lattice relaxation, because energy is exchanged with the surrounding media. T_1 is the time the macroscopic magnetization needs to return to the equilibrium (Curie) magnetization. The return to equilibrium is reached via the dissipation of energy to repositories for thermal energy, namely translation, rotation or vibration (the lattice).

A spread in the Larmor frequency because of magnetic field gradients (e.g. from paramagnetic ions in the rock matrix or inhomogeneities of the primary magnetic field) causes the relaxation signal to decrease to the relaxation time T_2^* (FID), given by

$$\frac{1}{T_2^*} = \frac{1}{T_2} + \gamma \nabla H_0, \tag{11}$$

where γ is the gyromagnetic ratio , ∇H_0 is the field gradient and $\gamma \nabla H_0$ is the distortion of the static magnetic field. When T_2^* is dominated by magnetic field inhomogeneities resulting from the primary field, T_2^* provides little information about the sample but more information on fundamental molecular processes, e.g. those that are intrinsic to the fluid. In liquids, experimental data show that T_1 almost equals T_2 (Fukushima and Roeder 1981). For the hydrogeophysical case, with fluids in porous media, this is no longer valid due to the interaction of the spin with local magnetic inhomogeneities.

NMR in porous media

The NMR relaxation times of fluids in porous media are shorter than for bulk fluids (pure fluid) due to the influence of the pore wall on the NMR relaxation. This influence is caused by local magnetic fields close to the pore surface. Similarly to the influence of neighbouring nuclei due to their local magnetic fields which causes the spins to relax, the pore wall is able to interact because it has also a local magnetic field. This magnetic field is about 1000 times stronger than the magnetic fields of the nuclei

(Watson and Chang 1997). Therefore the spins will relax much more quickly in the vicinity of the pore wall than in the bulk fluid (i.e. outside the range of influence of the pore wall, which decreases by the power of six with distance). The local magnetic field of the wall surface is mainly caused by paramagnetic materials of the grains that occupy sites (binding places) at the pore surface. The strength of this surface relaxation is described by the NMR surface relaxation parameter, ρ_{surf} [m/s].

Diffusion of the fluid molecules causes the spins to experience a change in magnetic field strength with place and time. The result is a faster relaxation time. The diffusion is dependent on the molecular diffusion constant D_0. By way of diffusion, spins that have been relaxed at the pore wall are transported to the inner pore and unrelaxed spins are transported to the surface where they can relax.

According to the different mechanisms of NMR relaxation, the following special relaxation times can be distinguished in porous media (Kenyon 1997):

- T^{surf} [s]: relaxation resulting from the pore-wall (pore-surface) contact (wall relaxation, WR);
- T^{bulk} [s]: bulk relaxation (BR) is measured in a fluid when wall and gradient effects are not present;
- T^{DR} [s]: relaxation is shortened by molecular diffusion in an inhomogeneous (gradient) static magnetic field (diffusion relaxation, DR);
- T^{PR} [s]: relaxation is shortened by the presence of paramagnetic materials such as manganese and iron (paramagnetic relaxation, PR). Paramagnetic materials of the matrix are the main contributors to wall relaxation, decreasing T^{surf}; paramagnetic molecules in fluids will shorten the bulk relaxation time, T^{bulk}.

Because the relaxation mechanisms work in parallel (Bloembergen *et al.* 1948), T_1 and T_2 relaxation time constants can be given by (Kenyon 1997)

$$\frac{1}{T_1} = \frac{1}{T_1^{bulk}} + \frac{1}{T_1^{surf}} \quad [1/s], \tag{12}$$

and

$$\frac{1}{T_2} = \frac{1}{T_2^{bulk}} + \frac{1}{T_2^{surf}} + \frac{1}{T_2^{DR}} \quad [1/s]. \tag{13}$$

It should be noted that, in contrast to the transverse relaxation time constant T_2, the longitudinal relaxation time constant T_1 is not affected by diffusion in a gradient field. The two key parameters of NMR surface relaxation are T^{surf} and the surface-to-pore-volume S^{por} (Kenyon 1997).

Water content (i.e. porosity) and pore size from NMR
For relating wall relaxation time to pore size, the porous medium can be characterized by the following geometrical parameters: the pore size a, which is equal to the quotient of the volume V and the surface area S of the pore ($a = V/S$), the cross-sectional area of a throat A_{pore}, and the distance between the centres of adjacent pores.

For the following, we assume that the molecular diffusion between pores can be neglected. Then the interpore coupling rate is small and the average distance of a water molecule and the centre of a nearby pore is large compared to the average distance between the water molecules and the pore. In this case DR<WR is true. Additionally the motion of the water molecules will be fast. In this so-called fast-diffusion limit, it can be proved that the relaxation in the pore can be written (Brownstein and Tarr 1977; Kenyon 1997; Watson and Chang 1997):

$$\frac{1}{T^{surf}} = \frac{1}{T^{bulk}} + \rho_{surf} \frac{S}{V_{por}} \quad [1/s]. \tag{14}$$

Note that either the bulk relaxation is considered to be insignificant or it can be removed by subtraction (equations (12) and (13)). When the parameter ρ_{surf} is known (for either T_1 or T_2), the pore size ($a = V/S$) can be calculated with the relaxation time and (14).

Sediments are characterized by a distribution of pore sizes instead of one single pore size (Kenyon 1997). The magnetization signal of the wall relaxation $M_s(t)$ can be written as the sum of the decaying signals for all pore sizes I,

$$M_s(t) = \sum_i A_i e^{-t/T_{1,2}^i}, \tag{15}$$

where A_i is the amplitude of the signal which is produced by the number of protons in pores of size i (amplitude of signal), T_1^i and and T_2^i are the decay time constants corresponding to T^{surf} in (14).

A so-called relaxation time distribution curve (or spectrum) is obtained by plotting A_i versus $T_{1,2}^i$ (equation (15)). According to (14), the relaxation-time distribution is related to the pore-size distribution curve provided that the fast-diffusion limit applies and each pore has its own relaxation time constant.

For completely saturated samples, the pore volume V_{por} is equal to the water volume $V_{H_2O}^{sample}$ of the sample, which is proportional to $M_z(t_0)$, the signal amplitude for $t = 0$, with

$$V_{H_2O}^{sample} \sim M_z(t_0) = \sum_i A_i. \tag{16}$$

$M_z(t_0)$ can be estimated by extrapolating the magnetization decay curve to zero time or by integration of the distribution curve.

The factor of proportionality can be determined by measuring the amplitude of a reference sample with an independently measured water volume, $V_{H_2O}^{reference}$. The water volume of the sample $V_{H_2O}^{sample}$ can be calculated from the equation:

$$V_{H_2O}^{sample} = \frac{A_{sample} V_{H_2O}^{reference}}{A_{reference}}. \tag{17}$$

When the pores of the sample are completely saturated then the porosity from NMR (ϕ_{NMR}) can be calculated from the equation:

$$\phi_{NMR} = \frac{V_{por}}{V} \ . \tag{18}$$

Permeability from NMR

The permeability k can also be derived from the NMR relaxation. The permeability from NMR relaxation has been estimated historically in three different ways:

1 estimation based on the irreducible water volume, $V_{w,irr}$ (after Timur 1968, 1969a,b):

$$k = \frac{\phi^4}{V_{w,irr}^2} \ ; \tag{19}$$

2 estimation based on porosity and the T_2 relaxation time constant (after Seevers 1966):

$$k = \phi (T_2)^2 \ ; \tag{20}$$

3 estimation based on porosity and the T_2 relaxation time constant and allowing for fitting for different sediment types (adjustment of the C-factor, after Kenyon 1997):

$$k = C\phi^4 (T_2)^2 \ . \tag{21}$$

Equations based on the pore size as determined by NMR are also used to estimate the permeability (Kenyon 1997):

$$a = \frac{V_{por}}{S} = \rho_{surf} T_1 \quad [m], \tag{22}$$

and this equation is squared to obtain the correct dimensions:

$$k = C a^2 = C(\rho_{surf} T_1)^2 \quad [m^2]. \tag{23}$$

In this case the permeability is not only a function of T_1 but also the surface relaxivity ρ_{surf}. In (23), however, information about the porosity is not explicitly included.

Equation (22) has been extended by including the formation factor, $F = \Phi/T$, in order to get a better estimation of permeability (Sen *et al*. 1990):

$$k = C\frac{1}{F^2} a^2 = C\frac{1}{F^2}(\rho_{surf} T_1) \quad [m^2]. \tag{24}$$

The factor F is the electrical formation factor defined by Archie (1942). Note that (23) can only be applied when the surface relaxivity is constant, otherwise estimates of the permeability will vary.

EXPERIMENTAL SET-UP
Sample material
All measurements were performed on samples that can be divided into five different groups (see also Table 1):

1 Synthetic samples consisting of small glass beads with three different diameters (0.1, 0.5 and 1.0 mm). Some of these are combined with clay. This group (group 1) has been taken as a control group; similar measurements have been conducted for glass beads in a previous study by Krüger (2001). The glass beads are industrial standard glass beads and are cleaned with distilled water to remove the polish used during the production process.

2 Clay samples made from pure clay. They were dried at 30°C and 60°C (ClayRoom and ClayDen, respectively) and pulverised with a Fritsch pulverisette.

3 Artificially-made sand mixtures. Samples consisting of different grain-size ranges were mixed (2–1, 1–0.5, 0.5–0.25, 0.25–0.125, 0.125–0.063, 0.063 mm). These samples were prepared in such a way that they are as close as possible to the Nauen samples (see Goldbeck 2002). This means that the grain spectra of the two samples are similar. The assumption is that, in this way, the properties of Nauen samples can be explained by artificial samples. As all fractions are mixed, the raw material has to be sieved to obtain the different grain size ranges: i.e. 0.063, 0.125, 0.25, 0.5, 1.0, 2.0 mm.

4 Artificially made sand mixtures with different clay contents of 3%, 5%, 10%, 15% and 20% by mass.

5 Samples taken from a bore core of a test site in the Nauen Quarternary deposits from west of Berlin, Germany (see also Yaramanci *et al*. 2002). The samples taken in this group are assumed to represent different hydrogeological regions in the subsurface of Nauen. Several geophysical methods have been applied to study the subsurface (Goldbeck 2002). This information was used to pick samples from the core (at depths of 15, 22, 23, 27 and 28 m) that represent the different hydrogeological regions, i.e. aquifer, aquitard.

Sample holder
In this research several different measurements were performed. In order to compare and correlate these measurements with each other, the same sample was used for all measurements. The limiting size of the sample is determined by the NMR spectrometer used (Maran Ultra 2 MHz, Resonance Instruments UK). The diameter of the measuring bore is about 5.1 cm (2''). The length about which the field of the permanent magnet is homogeneous is about 7 cm. The sample holder is made from macrolon tubes

TABLE 1

The five groups of samples and the individual samples they contain

Group	Samples in group
Group 1	S01, S05, S1, S1-05, S1-DENMIX, S!-DENLAY, S1-MIX, S1-LAY
Group 2	CLAYROOM, CLAYDEN
Group 3	SANCON1-SANCON3, SANCOA-1 to SAN-COA-5
Group 4	NAUEN B1-15, NAUEN B1-22, NAUEN B1-23, NAUEN B1-27, NAUEN B1-28
Group 5	3% CLAY, 5% CLAY, 10% CLAY, 15% CLAY, 20% CLAY

with four holes in it for electrodes to enable electrical measurements (SIP). The samples can be closed with plastic caps and duct tape to prevent evaporation and leakage.

Sample preparation

The sample holders were filled with material, and weighed in an oven-dry condition to obtain the dry weight. They were then saturated. In a first approach, the samples were saturated using an exsiccator device. This was done by evacuating all air out of the samples and then flooding the samples. This method has two disadvantages: (1) during the saturation process material is lost (the sample holders were almost filled to the top); (2) the amount of water that has entered the sample is unknown. Only after all the measurements were completed could the sample be dried and the weight loss measured by a balance. To reduce errors, the infiltration method was used: the water is injected with a needle until the sample is saturated. Excess water at the top of the sample is sucked away by a syringe. In this way the amount of water added is known precisely and most of the samples were saturated in this way. However, this method also has one disadvantage: the sample might appear to be saturated, but sometimes hidden air bubbles are trapped inside the sample. This problem can be overcome to a certain extent by gently tapping the sample on a hard surface; however, this only works for coarse materials. A better way is to use an ultrasonic bath that 'cuts' the air bubbles into small pieces so that they can escape via the pores more easily. This method (with a Bandelin Sonorex rk 100) was used to saturate the samples measured by the permeameter.

RESULTS

Porosity and specific surface

Figure 3 shows the relationship between the specific surface (S_{por}) and clay content for the samples in group 5. The relationship is almost one-to-one. The clay is the main source of the specific surface, not only for coarse sands but for all samples. Table 2 shows the petrophysical properties, such as specific surface, clay content, grain size, hydraulic conductivity, porosity and density. The porosities obtained from NMR agree reasonably well with the porosities measured with a pycnometer for most of the samples. The relaxation times become smaller in the progression from synthetic samples to sand mixtures and then to Nauen samples.

TABLE 2

Petrophysical parameters of samples: grain-size distribution and clay content (Grain sizes, Ratio), density (ρ), specific surface (S_{por}) from N_2 adsorption (BET), porosity from pycnometer (ϕ_{Pyc}), porosity from NMR (ϕ_{NMR}), hydraulic conductivity measured (k_f-Meas.), hydraulic conductivity calculated from T_1 (K–T_1), and hydraulic conductivity calculated from T_2 (K–T_2)

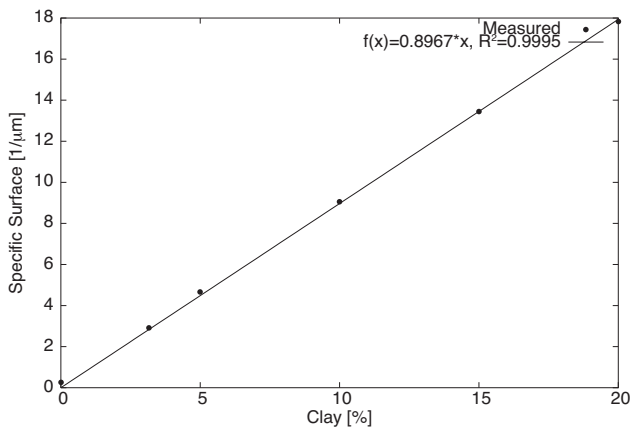| Sample	Grain sizes [mm]	Ratio [mass]	ρ [g/cm³]	S_{por} [1/μm]	ϕ_{Pyc}	ϕ_{NMR}	kf-Meas [m/d]	K-T2 [m/d]	K-T1 [m/d]
S01	0.1	1	2.53	1.01	0.39	0.35	20.78	7.22	15.67
S05	0.5	1	2.94	0.02	0.38	0.42	73.11	102.97	139.81
S1	1	1	2.53	0.01	0.37	0.38	199.26	494.00	492.87
ClayDen	<0.002	1	2.63	62.10	0.59	0.58	0.03	0.02	0.02
ClayRoom	<0.002	1	2.64	52.62	0.65	0.62	0.03	0.05	0.03
S1-05	1-0.5	1:1	2.72	0.02	0.34	0.37	136.95	142.52	130.68
S1-DENMIX	1-Den-Clay	1:1	2.40	-	-	0.49	-	-	-
S1-DENLAY	1-Den-Clay	1:1	-	-	-	0.56	-	-	-
S1-MIX	1-Clay	1:1	2.15	-	-	0.39	-	-	-
S1-LAY	1-Clay	1:1	-	-	-	0.51	-	-	-
SANCON1	1-0.5	1	2.64	0.42	0.37	0.40	108.07	97.52	93.03
SANCON2	1-0.5	1	2,64	0.42	0.37	0.40	108.95	92.16	78.45
SANCON3	1-0.5	1	2.64	0.42	0.37	0.42	120.56	58.74	78.61
SANCOA-1	0.125:0.25:0.5:1:2	18:42:36:2:2	2.65	0.47	0.35	0.37	1,41	15.20	36.91
SANCOA-2	0.063:0.125:0.25:0.5:1	3:20:69:7:1	2.66	0.42	0.40	0.42	0.61	28.43	70.02
SANCOA-3	0.125:0.25:0.5:1:2	7:28:41:17:4:3	2.66	0.66	0.37	0.42	1.78	20.15	49.06
SANCOA-4	0.063:0.125:0.25:0.5:1:2	70:20:4:3:2:1	2.66	18.77	0.51	0.51	0.56	0.08	0.09
SANCOA-5	0.063:0.125:0.25:0.5:1:2	65:20:8:4:2:1	2.66	20.93	0.50	0.48	1.19	0.10	0.09
NAUEN B1-15	0.125:0.25:0.5:1:2	17.8:42.1:36.1:1.4:0.4	2.66	1.12	0.36	0.29	3.04	26.46	14.92
NAUEN B1-22	0.063:0.125:0.25:0.5:1	2.6:19.8:68.3:7.3:0.5:0.7	2.66	2.51	0.40	0.36	0.34	26.68	5.94
NAUEN B1-27	0.063:0.125:0.25:0.5:1:2	7.1:26.6:41.0:16.2:4.2:2.5	2.66	2.02	0.37	0.37	3.27	8.02	1.32
NAUEN B1-28	0.063:.125:0.25:0.5:1:2	68.8:19.7:2.9:0.6:0.1:0.1	2.67	2.53	0.49	0.22	1.45	1.49	0.37
NAUEN B1-23	< 0.063:0.125:0.25:0.5:1:2	76.2:7.8:4.2:1.7:1.7:0.5	2.68	6.20	0.54	0.30	1.75	0.60	0.24

FIGURE 3

Specific surface (S_{por}) as function of clay content (%mass) of coarse sand samples (grain size 1.0–0.5 mm, group 5).
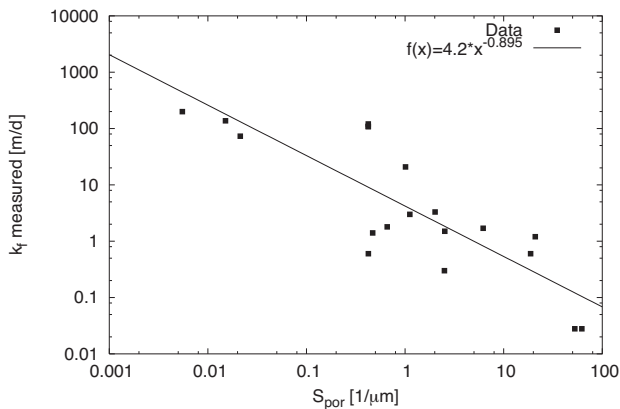

FIGURE 4

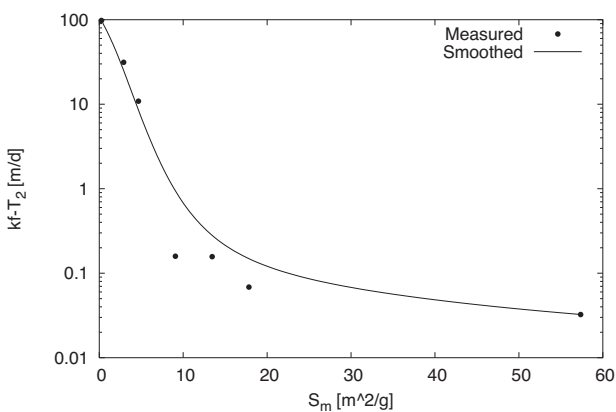Measured hydraulic conductivity k_f for all samples as a function of specific surface.

FIGURE 5

Hydraulic conductivity calculated from NMR- T_2 measurements versus specific surface S_m, for samples covering a range of clay content.

Hydraulic conductivity

The hydraulic conductivity measured on the coarse sand samples (group 5) shows an inverse relationship to the surface-to-pore-volume S_{por} (Fig. 4). Samples with a hydraulic conductivity between 0.7 and 3 m/d are more-or-less independent of the specific surface. This is comparable with the behaviour observed for samples which cover a range of clay contents (Fig. 5). Note that the hydraulic conductivity drops considerably in the specific surface range 0.2–5 m2/g. In contrast, the samples in the range 10–60 m2/g lie in a small range of hydraulic conductivity around 0.1 m/d. The data show that the relationship between specific surface and permeability is more complicated than expected from the Kozeny–Carman equation (equation (7)), if the specific surface results mainly from the clay content. Equation (21) in particular is not strictly valid. In this case, the individual structure on the mm scale plays a role and the relaxation mechanisms of both sample types, i.e. clean and shaly sands, might be completely different.

NMR vs. specific surface

The dependence of NMR decay times (T_1 and T_2) on specific surface is shown in Fig. 6. Most of the samples deviate within half an order of magnitude from the regression curve. The samples with a high silt and clay content lie below the regression line, whereas samples with a dominating sand fraction and a small amount of clay lie above the regression line. This can be explained by structural reasons: the diameter of the free-water compartment of a single large pore is not seriously reduced by a small amount of clay minerals. From (21) we should expect a reference line with a slope of –1. As the glass bead samples represent systems with a simple structure, we should adjust this reference line to the glass bead data. We then find that all sand/clay mixtures lie above this line, which means that for these samples the NMR decay times indicate larger pore voids than expected from the specific surface, which is mainly due to the clay minerals.
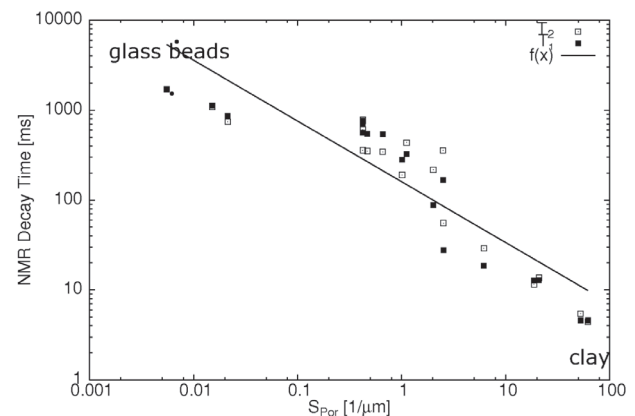

FIGURE 6

NMR decay time T_1 (solid squares) and T_2 (open squares) as a function $f(x)$ of specific surface; $f(x) = 160^*x^{-0.68}$.

NMR decay-time and pore-size distribution

Figure 7 shows the pore-size distribution derived from the relaxation-time distribution for a layered sample (glass beads on top of clay). Separate peaks are resolved for clay and for glass beads, i.e. both materials behave independently. However, when the same materials are mixed together, only the clay peak is observed with a mean relaxation-time constant equal to that of pure clay (see Fig. 8). In this way the glass beads are 'masked' and unobservable by NMR alone. Combination with SIP measurements may be helpful in this case (Müller and Yaramanci 2004).

NMR vs. hydraulic conductivity

The relationship between hydraulic conductivity from NMR and specific surface for samples which cover a range of clay contents is shown in Fig. 5 and discussed above. The hydraulic conductivity shows a fast decay for clean samples and a slight decay for shaly sands and clays as the specific surface (S_m) increases. The results are in accordance with measurements on similar samples by Slater and Lesmes (2002).

The hydraulic conductivities calculated from NMR show good agreement with the measured hydraulic conductivities for the clayey samples and the glass beads (Fig. 9). However, the calculated values for the other samples deviate by up to two orders of magnitude from the measured values. Here, we can distinguish between two groups of samples, the clayey sand samples of Nauen, together with the Nauen-like mixtures, and the silty samples, Sancoa-4 and Sancoa-5. The Nauen samples are characterized by relaxation times and calculated hydraulic conductivities that are too high for their measured hydraulic conductivity, and the relaxation times are higher than expected for their specific surface (see Fig. 6). This can be explained by a structure in which the clay leaves large voids in the pores, which corresponds to large relaxation times. On the other hand, clay may clog the pore throats or may separate into layers, which reduces permeability. In contrast, the calculated hydraulic conductivities of the silty samples are smaller than the measured values.

The difference between the calculated hydraulic conductivities for the Kozeny–Carman (equation (7)) and Hazen (equation (8)) models is a maximum of three orders of magnitude for low hydraulic conductivities and about one order of magnitude for high hydraulic conductivities (Fig. 10). A comparison of the estimated and measured hydraulic conductivities as a function of specific surface shows that the Hazen model fits the data better than the Kozeny–Carman model (Fig. 11).

Laboratory NMR vs. SNMR – dispersion of relaxation

To investigate if and how NMR parameters measured in the laboratory can be used to interpret (SNMR) field data, we compiled laboratory and field data for different grain sizes. Table 3 shows relaxation data at different precession frequencies. Data at 2 MHz and 400 MHz are laboratory measurements, data at 2 kHz were obtained from SNMR field measurements.
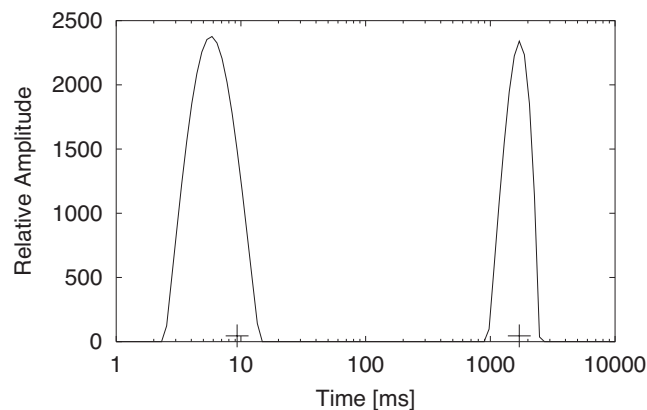

FIGURE 7

Decay-time distribution of a layered sample with glass beads on top of clay (S1-Denlay). The crosses indicate the decay times for a two-exponential fit of the same data.
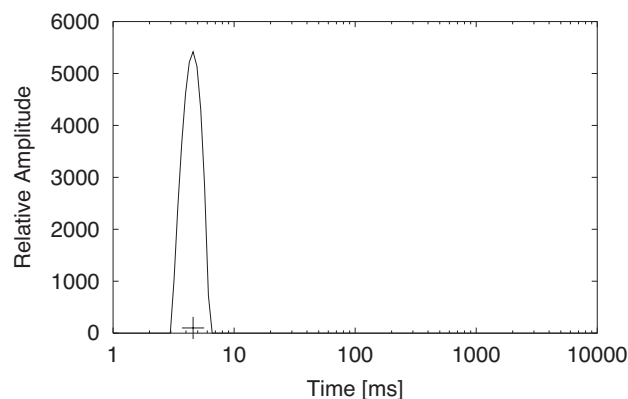

FIGURE 8

Decay-time distribution of sample with clay and glass beads mixed (S1-Denmix). The cross in the figure indicates the mean relaxation time.
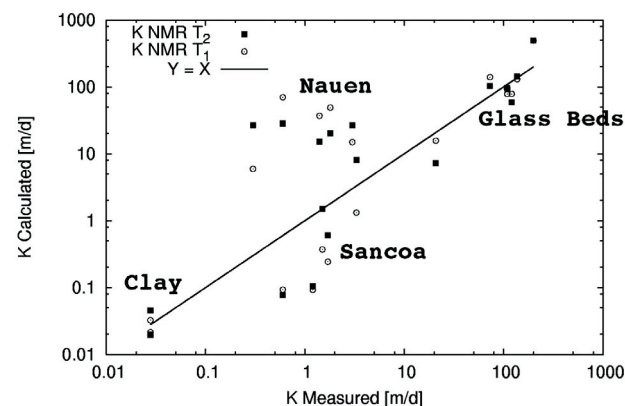

FIGURE 9

Hydraulic conductivities calculated from NMR decay times versus measured hydraulic conductivities obtained with a permeameter.
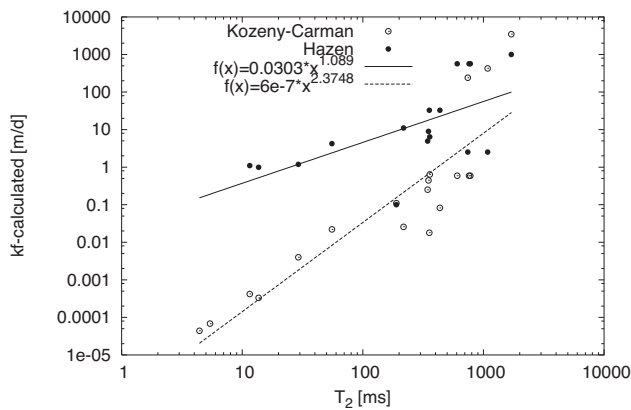
FIGURE 10
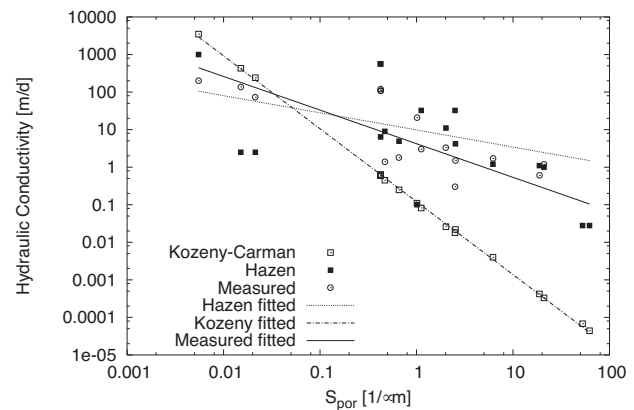Hydraulic conductivity estimated with Kozeny–Carman and Hazen models as function of NMR-T_2 decay time.

FIGURE 11
Hydraulic conductivity (measured and estimated) as a function of surface-to-pore volume S_{por}.

TABLE 3

T_1, T_2 and relaxation data acquired at different Larmor frequencies. The data from Shirov et al. (1991)[1], Legchenko et al. (2002)[2] and Mohnke and Yaramanci (2002)[6] have been derived from SNMR measurements; the data from Müller et al. (2002)[3] and this work[4] at 2 MHz, and from Willamowski (1997)[5] at 400 MHz were obtained from laboratory measurements. The superscripts denote the above references

Relaxation [ms]								
	2 kHz (SNMR)		2 MHz			400 MHz		
Sediment type	T_2^*	T_1	T_2^*	T_2	T_1	T_2^*	T_2	T_1
Clay	-	-	0.4-0.7[4]	4-6[4]	4-5[3,4]	0.01[5]	4[5]	11[5]
Silt	-	-	0.5[4]	12-14[4]	13[4]	-	-	-
Sandy clay	<30[1]	-	-	-	-	-	-	-
Clayey/very fine sand	30-60[1]	-	0.2-0.8[4]	30-55[4]	20-30[4]	-	-	-
Fine sand	60-120[1]	310[2]	0.4-1.3[4]	10-435[4]	90-560[4]	-	-	-
Medium sand	120-180[1,6]	420[2,6]	0.7[4]	220[4]	540[4]	0.05[5]	2[5]	530[5]
Coarse/gravelly sand	180-300[1,6]	600[2,6]	0.5-0.8[4]	600-800[4]	700-760[4]	-	-	-
Gravel	300-600[1]	-	-	-	-	-	-	-
Surface water	600-1500[1]	-	0.9[3,4]	-2500[3]	3000[3]	-	-	-

- The coarser the material, the slower is the relaxation for T_1 and T_2 for all frequencies.
- Only for small field strengths (2 kHz) does the T_2^* relaxation shows a clear dependence on the grain size, like T_1 and T_2.
- The higher the Larmor frequency, the shorter is the T_2^* relaxation time: for medium sand, it is ~150 ms for 2 kHz, ~1 ms for 2 MHz and 0.05 ms for 400 MHz. This is due to the effect of increasing magnetic field gradients and therefore increasing dephasing in the Lamor frequency with higher field strengths.
- Comparing T_2 for medium sands at 2 MHz and 400 MHz shows that magnetic field gradients also apparently have a strong influence, as T_2 at 2 MHz is 200 times larger than at 400 MHz.
- Comparing T_1 at different Lamor frequencies shows that not only the 2 MHz and the 400 MHz values coincide well, but also that for 2 kHz.
- Comparing T_2^* (SNMR) at 2 kHz and T_2 at 2 MHz (laboratory) shows that there is a 1:1 correlation for material finer than medium sand. For material coarser than medium sand, a 'relaxation shift' for SNMR T_2^* towards 2 MHz T_2 of a factor of 1.5–2 must be taken into account, but this may depend on the presence of paramagnetic nuclei in the sample.

DISCUSSION AND CONCLUSIONS

The hydraulic conductivities calculated from NMR show good agreement with the measured hydraulic conductivities for the clayey samples and the glass beads (Fig. 9). The coarse sand samples (Sancoa-1, -2 , -3 and Nauen B1-15, B1-22 and B1-27) show a 'too high' calculated hydraulic conductivity. It seems that

the large pores determine the mean relaxation time, but for the 'true' hydraulic conductivity, the poor sorting of the sample is important (poor sorting decreases the hydraulic conductivity). Straley *et al.* (1997) found a pre-factor (*C* in equation (23)) of about 4.6 for sandstones. In this work a factor of 1 was applied, and this provides a good fit for clay and coarse materials. Another possible explanation of the scatter in hydraulic conductivity is the variation of surface relaxivity between the samples. The glass beads, as already discussed, have a lower specific surface than natural material, which explains the long relaxation time. The natural samples consist of material of different origins: clean sands with a low amount of paramagnetic material (group 3) and sands that might be covered with a paramagnetic 'skin' (group 4). Because of its strong magnetic influence only a small amount of paramagnetic material is sufficient to have a significant influence on the relaxation time.

The hydraulic conductivity estimated by the Hazen model is much closer to the 'true' hydraulic conductivity than the more sophisticated Kozeny–Carman model. The failure of the Kozeny–Carman model results from the fact that two different values of specific surface are used: the one that is measured with a special method and the one that is responsible for a physical process, both depend on their individual resolution power and may be different. When using the Kozeny–Carman model, the specific surface values measured by nitrogen adsorption have to be converted to smaller values which correspond to the smoother surfaces involved in hydraulic flow and in NMR relaxation (Pape *et al.* 1999, 2000). The estimation of both models is better for higher hydraulic conductivities (sand instead of clay or silt). Both models are developed to estimate the hydraulic conductivity of sandy samples. Thus the result is not surprising. Similar results for the Kozeny–Carman and Hazen models were obtained by Slater and Lesmes (2002). They also found that a Hazen-type equation provides hydraulic conductivity estimates that differ by an order of magnitude from the measured hydraulic conductivity and that for poorly sorted materials the estimation is the poorest.

The compiled laboratory and field relaxation data are in good agreement with the results of SNMR-T_1 and SNMR-T_2^* surveys using measurements taken in Haldensleben (Yaramanci *et al.* 1999) and Nauen (Mohnke and Yaramanci 2002), where values of 155 ms for T_2^* for grain sizes between 0.1 and 1 mm correspond to values of 300–400 ms for T_1. To summarize: firstly, it becomes clear that SNMR-T_1 values compare well with T_1 values acquired in the laboratory, not only at 2 MHz but also for higher field strengths. Secondly, the SNMR-T_2^* values cannot be compared with T_2^* data from the laboratory for any frequency because of dephasing effects. Thirdly, it is not always necessary to perform SNMR-T_1 surveys to obtain 'good' relaxation data to derive pore properties. Instead, SNMR-T_2^* values can be compared to T_2 values from laboratory NMR with a certain correction (rule-of-thumb) factor of 1.5–2. This may be no longer valid in survey areas which exhibit large magnetic inhomogenieties or large concentrations of magnetic minerals.

Besides deeper understanding of the dispersion of relaxation mechanism, further work should focus on gathering additional experimental data, for example, by

- performing 2 kHz laboratory experiments;
- performing experiments at intermediate (logging tool) field strengths (e.g. 500 kHz);
- enhancing the quality of hydraulic conductivity measurements of samples in the laboratory, e.g. by the use of larger samples;
- including field hydraulic conductivity measurements, e.g. from pumping tests.

Finally we intend to establish a comprehensive database of NMR/SNMR relaxation times, including those from samples/rocks, in order to integrate SNMR-user knowledge. This database should include not only the NMR parameters, but also additional hydrogeophysical parameters, such as porosity, hydraulic conductivity and salinity. Müller and Yaramanci (2004) showed recently how the combination of SIP and NMR can enhance interpretation significantly.

ACKNOWLEDGEMENTS

REFERENCES

Abragam A. 1983. *Principles of Nuclear Magnetism*, pp. 297–309, 63–65. Oxford University Press.

Archie G. 1942. The electrical resistivity log as an aid in determining some reservoir characteristics. *Transactions of the American Institute of Mining Metallurgy and Engineering* **146**, 54.

Bear J. 1972. *Dynamics of Fluids in Porous Media*. American Elsevier Publishing Co., New York.

Bené G.J. 1980. Nuclear magnetism of liquid systems in the earth field range. *Physics Reports* **58**(4), 213–267.

Bloembergen N., Purcell E.M. and Pound R.V. 1948. Relaxation effects in nuclear magnetic resonance absorption. *Physics Review* **73**, 679–712.

Brownstein K.R. and Tarr C.E. 1977. Spin-lattice relaxation in a system governed by diffusion. *Journal of Magnetic Resonance* **26**, 17–24.

Fukushima E. and Roeder B.W. 1981. *Experimental Pulse NMR*. Addison–Wesley Publishing Co.

Goldbeck J. 2002. *Hydrogeophysical measurements at the test-site Nauen – evaluation and optimization*. MSc thesis, Technical University, Berlin.

Hölting B. 1989. *Hydrogeologie*. 3rd edition. Enke Verlag, Stuttgart.

Kenyon W. 1997. Petrophysical principles of applications of NMR logging. *The Log Analyst* **38** (2), 21–43.

Krüger U. 2001. *Untersuchungen mit der Nuklearmagnetischen Resonanz (NMR) an Gesteinsproben und synthetischen Materialien*. MSc. thesis, Technical University, Berlin.

Legchenko A.V., Baltassat J.-M., Beauce A. and Bernard J. 2002. Nuclear magnetic resonance as a geophysical tool for hydrogeologists. *Journal of Applied Geophysics* **50**, 21–46.

Legchenko A.V. and Beauce A. 1999. Surface proton magnetic resonance method: What do users get? *Proceedings of 5th Meeting of the Environmental and Engineering Geophysics, European Section*, Budapest, pp. ?

Legchenko A.V. and Shushakov O.A. 1998. Inversion of surface NMR data. *Geophysics* **63**, 75–84.

Legchenko A.V. and Valla P. 2002. A review of the basic principles for proton magnetic resonance sounding measurements. *Journal of Applied Geophysics* **50**, 3–19.

Mohnke O. and Yaramanci U. 2002. measurements with surface nuclear magnetic Resonance – realisation and assessment. *Proceedings of EEGS-ES*, Aveiro, Portugal, pp. 559–562.

Müller M., Krüger U. and Yaramanci U. 2002. Nuclear magnetic resonance (NMR) properties of unconsolidated rocks and synthetic samples. *Proceedings of EEGS-ES*, Aveiro, Portugal, pp. 339–342.

Müller M. and Yaramanci U. 2004. Interpretation enhancement by combining SIP and NMR. *Proceedings of 10th European Meeting on Environmental and Engineering Geophysics*, Utrecht, NL, paper A006.

Pape H., Clauser C. and Iffland J. 1999. Permeability prediction for reservoir sandstones based on fractal pore space geometry. *Geophysics* **64**, 1447–1460.

Pape H., Clauser C., Iffland J. 2000. Permeability-porosity relationship in sandstone based on fractal pore space geometry. *Pure and Applied Geophysics* **157**, 603–619.

Schön J.H. 1996. *Physical Properties of Rocks: Fundamentals and Principles of Petrophysics*. Vol. 18 of *Handbook of Geophysical Exploration*. Sect. 1; Vol. 18. Elsevier Science Publishing Co., Pergamon Press.

Seevers D.O. 1966. A nuclear magnetic method for determining the permeability of sandstones. *Transactions of SPWLA*, Paper L 24.

Sen P., Straley C., Kenyon W. and Whittingham M. 1990. Surface-to-volume ratio, charge density nuclear magnetic relaxation, and permeability in clay-bearing sandstones. *Geophysics* **55** , 61–69.

Shirov M., Legchenko A. and Creer G. 1991. A new direct non-invasive groundwater detection technology for Australia. *Exploration Geophysics* **22**, 333–338.

Slater L. and Lesmes D.P. 2002. Electrical-hydraulic relationships observed for unconsolidated sediments. *Water Resources Research* **38** (10), 1–13.

Straley C., Rossini D., Vinegar H., Tutunjian P. and Morriss C. 1997. Core analysis by low-field NMR. *The Log Analyst* **38** (2), 84–94.

Timur A. 1968. An investigation of permeability, porosity and residual water saturation relationships. *Transactions of the Society of Professional Well Log Analysts*: Annual Logging Symposium, Paper k.

Timur A. 1969a. Producible porosity and permeability of sandstones investigated through nuclear magnetic resonance principles. *The Log Analyst* **10**(1), 3–11.

Timur A. 1969b. Pulsed nuclear magnetic resonance studies of porosity, moveable fluid, and permeability of sandstones. *Journal of Petroleum Technology* **21**, 775–786.

Watson A.T. and Chang C.T.P. 1997. Characterizing porous media with NMR methods. *Progress in Nuclear Magnetic Resonance Spectroscopy* **31** (4), 343–386.

Willamowski S. 1997. *NMR im Erdfeld*. PhD thesis, University of Dortmund.

Yaramanci U., Lange G. and Hertrich M. 2002. Aquifer characterisation using Surface NMR jointly with other geophysical techniques at the Nauen/Berlin test site. *Journal of Applied Geophysics* **50**, 47–65.

Yaramanci U., Lange G. and Knödel K. 1999. Surface NMR within a geophysical study of an aquifer at Haldensleben (Germany). *Geophysical Prospecting* **47**, 923–943.